

available at [www.sciencedirect.com](http://www.sciencedirect.com)journal homepage: [www.ejconline.com](http://www.ejconline.com)

# Interaction between human-breast cancer metastasis and bone microenvironment through activated hepatocyte growth factor/Met and $\beta$ -catenin/Wnt pathways

Sara Previdi <sup>a,d</sup>, Paola Maroni <sup>b,d</sup>, Emanuela Matteucci <sup>c</sup>, Massimo Brogginì <sup>a</sup>, Paola Bendinelli <sup>c</sup>, Maria Alfonsina Desiderio <sup>c,\*</sup>

<sup>a</sup> Istituto di Ricerche Farmacologiche “Mario Negri”, Milano, Italy

<sup>b</sup> Istituto Ortopedico Galeazzi-IRCCS, Milano, Italy

<sup>c</sup> Dipartimento di Morfologia Umana e Scienze Biomediche “Città Studi”, Molecular Pathology Laboratory, Università degli Studi di Milano, Milano, Italy

## ARTICLE INFO

### Article history:

Received 10 November 2009

Received in revised form 21 January 2010

Accepted 23 February 2010

Available online 29 March 2010

### Keywords:

HGF

Met receptor

Bone-breast cancer metastases

$\beta$ -Catenin

Tumour microenvironment

## ABSTRACT

To clarify the reciprocal interaction between human-breast cancer metastatic cells and bone microenvironment, we studied the influence of HGF/Met system on a proposed-prognostic marker of aggressiveness, the  $\beta$ -catenin/Wnt pathway. For *in vitro* and *in vivo* experiments we used 1833-bone metastatic clone, derived from human-MDA-MB231 cells. In osteolytic bone metastases and in metastatic cells, Met was expressed in nuclei and at plasma membrane, and abnormally co-localised at nuclear level with  $\beta$ -catenin and the tyrosine phosphorylated c-Src kinase. Thus, in 1833 cells nuclear-Met COOH-terminal fragment and  $\beta$ -catenin-TCF were constitutively activated, possibly by receptor and non-receptor tyrosine kinases. The activity of the gene reporter TOPFLASH (containing multiple TCF/LEF-consensus sites) was measured, as index of  $\beta$ -catenin functionality. In 1833 cells, human and mouse HGF increased Met and  $\beta$ -catenin tyrosine phosphorylation and expression in nuclear and perinuclear compartments,  $\beta$ -catenin nuclear translocation via Kank and TOPFLASH transactivation. Human HGF was autocrine/intracrine in bone metastasis, and mouse HGF originating from the adjacent host-bone marrow, was found inside the metastatic nuclei. Parental MDA-MB231 cell nuclei did not show functional  $\beta$ -catenin, for TCF-transactivating activity, and the regulation by HGF. Our study highlighted the importance of the metastasis-stroma interaction in human-breast cancer metastatisation and first identified the HGF/nuclear Met/phospho-c-Src/ $\beta$ -catenin-TCF/Wnt pathway as a potential-therapeutic target to delay establishment/progression of bone metastases by affecting the aggressive phenotype.

© 2010 Elsevier Ltd. All rights reserved.

## 1. Introduction

The skeleton is the preferred site of breast-cancer metastasis, the principal cause of death for tumours in Western women. The major focus of breast cancer research is to identify criti-

cal molecular events in metastatisation for improving clinical management of metastatic disease.<sup>1–4</sup>

Bone microenvironment controls the vicious cycle of metastasis growth and bone destruction, and alters metastatic-cell phenotype giving highly aggressive lesions.

\* Corresponding author. Address: Università degli Studi di Milano, Dipartimento di Morfologia Umana e Scienze Biomediche “Città Studi”, Molecular Pathology Laboratory, via Luigi Mangiagalli, 31, 20133 Milano, Italy. Tel.: +39 0250315334; fax: +39 0250315338.

E-mail address: [a.desiderio@unimi.it](mailto:a.desiderio@unimi.it) (M.A. Desiderio).

<sup>d</sup> These authors contributed equally to this work.

0959-8049/\$ - see front matter © 2010 Elsevier Ltd. All rights reserved.

doi:10.1016/j.ejca.2010.02.036

Breast-cancer metastasis stimulates osteolysis, and the consequent release of numerous growth factors (TGF- $\beta$ , IGFs, FGF, PDGF, bone morphogenetic protein) immobilised within the bone matrix: they directly stimulate metastatic cell proliferation, and indirectly seem to promote angiogenesis and production of osteolytic and osteoblastic factors.<sup>2</sup>

The implication of other biological signals in the pathogenesis of bone metastasis is not completely clear. Since hepatocyte growth factor (HGF)/Met receptor system regulates various aspects of invasive growth *in vitro* and *in vivo*,<sup>1,5,6</sup> we hypothesised its critical role in human-breast cancer metastatisation to bones that has been scarcely investigated.

In the present translational research we used a xenograft model generated with human 1833-bone metastatic clone, derived from MDA-MB231 cells,<sup>7</sup> to better understand the implication of deregulated HGF/Met system and its crosstalk with bone microenvironment in the formation of osteolytic metastases. The model reproduces the most common type of breast-cancer metastasis in patients. The use of innovative imaging techniques, such as bioluminescence optical imaging (BLI) and micro-computed tomography ( $\mu$ -CT), allowed us to properly study *in vivo* bone-metastasis engraft, growth and osteolysis.

The novelty of our study consists in evaluating the role of the multifunctional-cytokine HGF since tumour-stroma interaction might increase HGF production, influencing bone metastatisation of human-breast carcinoma, and 'anti-cytokine' medicine is a rapidly growing field with major pharmaceutical impact.

The aim was to define the functional significance of HGF/Met system in relation to the  $\beta$ -catenin/Wnt pathway, a proposed-prognostic marker of metastases progression that also participates in stemness maintenance,<sup>8–11</sup> and until now studied mostly for bone metastases from prostate carcinoma.<sup>12</sup> It can be supposed that HGF affects the metastatic-cell homing, consistent with our findings that HGF reduces CXCR4 and Met expression through histone deacetylation in human invasive/metastatic MDA-MB231 breast carcinoma cells.<sup>13</sup> Also, HGF/Met system may influence extravasation/angiogenesis, because of activation of HIF-1/NF- $\kappa$ B network of transcription factors in the 1833 cells<sup>14</sup>; among the gene targets there are VEGF and MMPs 1, 2 and 9.<sup>2,6,15,16</sup> Other steps of the metastatic process might be influenced by HGF/Met through the regulation of  $\beta$ -catenin-TCF transcription factor target genes, such as cyclin D1 for growth control, different MMPs for invasiveness and osteopontin for osteolysis.<sup>12,17–19</sup>

Beyond availability of HGF, paracrine and sometimes autocrine in tumours,<sup>20,21</sup> expression level and autophosphorylation of Met control the triggering of downstream-signal pathways. Met is rarely activated through mutation(s) in tumours.<sup>5,22</sup> Met activation or over-expression, i.e. enhanced transcription or gene amplification, correlates with poor prognosis in tumour patients.<sup>22</sup> In breast cancer, Met over-expression is associated with death caused by metastatic disease.<sup>23</sup> Active intranuclear COOH-Met fragments regulate invasiveness of aggressive-human-breast cancer cells.<sup>24</sup>

We found an abnormally active  $\beta$ -catenin/Wnt signalling pathway *in vitro* and *in vivo* in metastasis, because of the aberrant nuclear expression of active  $\beta$ -catenin and elevated TCF-

transactivating activity. In the nuclear compartment of metastatic cells  $\beta$ -catenin seemed to be constitutively tyrosine phosphorylated by phospho-COOH-Met and phospho-c-Src, also in response to autocrine/intracrine HGF. After the arrival in the secondary growth site, HGF produced by bone marrow seemed to further enhance  $\beta$ -catenin/TCF signalling pathway by increasing  $\beta$ -catenin translocation to the nucleus and phosphorylation.

## 2. Materials and methods

### 2.1. Materials

Recombinant-human and recombinant-mouse HGF, anti-mouse HGF antibody, human-HGF immunoassay (ELISA) were from R&D System (Abingdon, UK). Anti-human HGF $\alpha$  (H487) antibody was from Immuno-Biological-Laboratories Inc. (Minneapolis, MN, USA). Antibodies for human Met (C12), glycogen-synthase kinase 3 $\beta$  (GSK3 $\beta$ ) (0011-A), phospho-GSK3 $\beta$  (Ser9); antibodies for c-Src (SRC2) and  $\beta$ -catenin (H-102) for immunoprecipitation and anti-vinculin antibody were from Santa-Cruz Biotechnology (Santa Cruz, CA, USA). Anti-phospho-Met (Tyr1234/1235) and anti-phospho-tyrosine Alexa Fluor568-conjugated antibodies were from Cell-Signaling Technology (Beverly, MA, USA). Anti- $\beta$ -catenin (610153) antibody for immunofluorescence and Western blot was from BD-Transduction Laboratories (Franklin Lakes, NJ, USA). Anti-c-Src (clone GD11) for Western blot, anti-phospho-c-Src (Tyr416, clone 9A6), anti-phospho-c-Src(Tyr416)-Alexa Fluor488 conjugated, anti-phosphotyrosine (4G10) antibodies were from Upstate Biotechnology (Lake Placid, NY, USA). Anti-human-cytokeratin antibody (clone MNF-116) was from DAKO (Glostrup, Denmark). Anti-Kank monoclonal antibody (clone 12A) was kindly given by R. Kiyama (Ibaraki, Japan).

### 2.2. Cells

Parental-MDA-MB231 cells, the derived bone-metastatic clone 1833 wild-type and retrovirally transfected with the triple reporter construct (1833/TGL)<sup>7,25</sup> were maintained in DMEM containing 10% (v/v) FBS (Sigma-Aldrich, St. Louis, MO, USA). Treatments with recombinant-human HGF (100 ng/ml) or recombinant-mouse HGF (from 50 to 200 ng/ml) were performed 24 h after starvation.

### 2.3. Immunoprecipitation and Western blot

Total and nuclear extracts from cells exposed or not to HGF were used for Western blot (100  $\mu$ g of total and 50  $\mu$ g of nuclear proteins) or immunoprecipitated (1 mg of total and 500  $\mu$ g of nuclear proteins) with the antibody for Met (6.5  $\mu$ g), c-Src (5  $\mu$ g) or  $\beta$ -catenin (3  $\mu$ g).<sup>24,26</sup> Densitometric analysis was performed after reaction with ECL- or ECLplus-chemiluminescence kit (GE Healthcare, Milan, Italy).

### 2.4. Fluorescence microscopy

The cells ( $8 \times 10^4$ ) on coverslips, exposed to HGF, were probed with the indicated antibodies. The images were collected at

400× magnification under Eclipse 80i, Nikon fluorescence microscope.<sup>24</sup>

## 2.5. Plasmids and cell transfection

The cells were transfected with TOPFLASH- or FOPFLASH-gene reporter from B.M. Gumbiner (Memorial Sloan-Kettering Cancer Center, NY, USA),<sup>27</sup> or with  $\beta$ -catenin promoter-containing construct (pSEAPBhBCTNf3) (BCCM/LMBP, Belgium), subcloned in PGL2 enhancer. The furnished p-SEAPbasic construct was cut with PstI, filled with Klenow-polymerase and then cut with XhoI; PGL2 enhancer was cut with HindIII, filled with Klenow-polymerase and then cut with XhoI to insert the  $\beta$ -catenin-promoter fragment. As internal control, Renilla-luciferase plasmid was co-transfected in the cells, and Firefly/Renilla luciferase activity ratios were calculated by the software.

## 2.6. Bone-metastasis xenograft model

Female-athymic 4-week-old nude mice (Harlan-Italy, Udine, Italy) were used. Procedure involving animals and their care were in conformity with the institutional guidelines, in compliance with national and international laws and policies. Mice, anesthetised with 0.2 ml/10 g body weight Avertin (Sigma-Aldrich), were injected in the heart with  $5 \times 10^5$  1833/TGL cells or saline (controls).<sup>7</sup> Firefly D-luciferin (150 mg/kg i.p.) was given under anaesthesia. Photon emission as pseudo-colour images was recorded with Explore Optix System (ART-Advanced Research Technologies, Montreal, Canada). Upon bioluminescent signal detection in hind-limb bone (10–12 d after cell injection), the mice were randomised into two groups, each of 8 animals, and sacrificed at 20 and 28 d from cell injection. The mice were monitored with  $\mu$ -CT to examine osteolysis using a cone-beam  $\mu$ -CT scanner (eXplore Locus; General Electric Healthcare, Milan, Italy). The scan parameters for non-gated scan acquisitions were: 80 kV peak, 450  $\mu$ A current, 100 ms per frame and 93  $\mu$ m of spatial resolution. After scanning, three-dimensional images obtained from axial, sagittal and coronal  $\mu$ -CT projections were reconstructed using MicroView software (General Electric Healthcare).

## 2.7. Histology

Femurs and tibia, excised from control and 1833/TGL-injected animals at days 20 and 28, were fixed and decalcified in Mielodec (Bio-Optica, Milan, Italy), dehydrated, embedded in paraffin. H&E staining was performed by standard protocol.

## 2.8. Immunohistochemistry

Serial sections from bones of control and 1833/TGL-injected mice, and surgical specimens of human-breast cancer were used. Patients provided informed consent in accordance with Declaration of Helsinki. After antigen retrieval (95 °C for 20 min at pH 6 in antigen-unmasking solution, Vector Laboratories, Burlingame, CA, USA), sections were treated for 10 min with 0.1% (v/v) H<sub>2</sub>O<sub>2</sub> and blocked with serum. Used-antibody dilutions: anti-human-cytokeratin (1:300, 1 h at room temper-

ature); anti-mouse HGF (10  $\mu$ g/ml overnight at 4 °C); anti-human HGF $\alpha$  (3  $\mu$ g/ml overnight at 4 °C); polyclonal anti- $\beta$ -catenin (1:50 overnight at 4 °C); anti-Met (1:100, 1 h at 37 °C).<sup>28</sup> Immunostaining was performed with a streptavidin-biotin system (ABC kit, Santa-Cruz Biotechnology) and diaminobenzidine substrate; counterstaining was with Meyer's haematoxylin. Negative-control sections were subjected to the same staining procedure without the primary antibody. Slides were visualised under BX60-Olympus microscope.

## 2.9. Human-HGF ELISA

HGF was measured in conditioned medium of 1833 cells, cultured for 72 h without FBS, and in the serum of metastasis-bearing animals with Quantikine Immunoassay (R&D System), following manufacturer's protocol.

## 2.10. Statistical analysis

Luciferase activity and densitometric values were analysed by analysis of variance, with  $P < 0.05$  considered significant. Differences from controls were evaluated on original experimental data.

# 3. Results

## 3.1. HGF is involved in $\beta$ -catenin expression, localisation and TCF-transactivating activity in 1833 cells

To evaluate the role of  $\beta$ -catenin/Wnt signalling pathway in breast-cancer metastasis and the influence of HGF/Met system, the bone-metastatic clone 1833 and the parental MDA-MB231 cells were examined. As shown in Fig. 1A, Met and  $\beta$ -catenin signals were prevalently in the nuclei of 1833 starved cells, even if Met was present throughout the cell.<sup>24</sup> HGF treatment seemed to increase the expression and to affect the distribution of  $\beta$ -catenin, that co-localised with enhanced Met in nuclear and perinuclear (cytosolic) compartments. In MDA-MB231 starved cells, Met and  $\beta$ -catenin were present in nuclei and cytosol and were practically unaffected by HGF exposure.

Both receptor (Met) and non-receptor (c-Src) tyrosine kinases might phosphorylate  $\beta$ -catenin, causing its activation.<sup>27–30</sup> c-Src may be directly phosphorylated downstream of HGF/Met.<sup>4</sup> In 1833-cell nuclei, phospho-c-Src (pSrc) and  $\beta$ -catenin signals remarkably co-localised under basal conditions (Fig. 1B). HGF enhanced nuclear pSrc and  $\beta$ -catenin signals and increased, therefore, the intensity of the merge III image. In MDA-MB231-starved cells pSrc was perinuclear, and co-localised with  $\beta$ -catenin in the cytosol after HGF.

Next, we examined whether HGF exposure transcriptionally regulated  $\beta$ -catenin level and/or affected  $\beta$ -catenin stability triggering  $\beta$ -catenin/Wnt pathway, evaluated as TCF-transactivating activity. MDA-MB231 and 1833 cells were transiently transfected with  $\beta$ -catenin-gene reporter, containing the sequence –4700 to +1300 that includes the promoter, the first exon and part of the first intron.<sup>8</sup> Only in 1833 cells luciferase activity was enhanced (3-fold) by HGF treatment (data not shown).

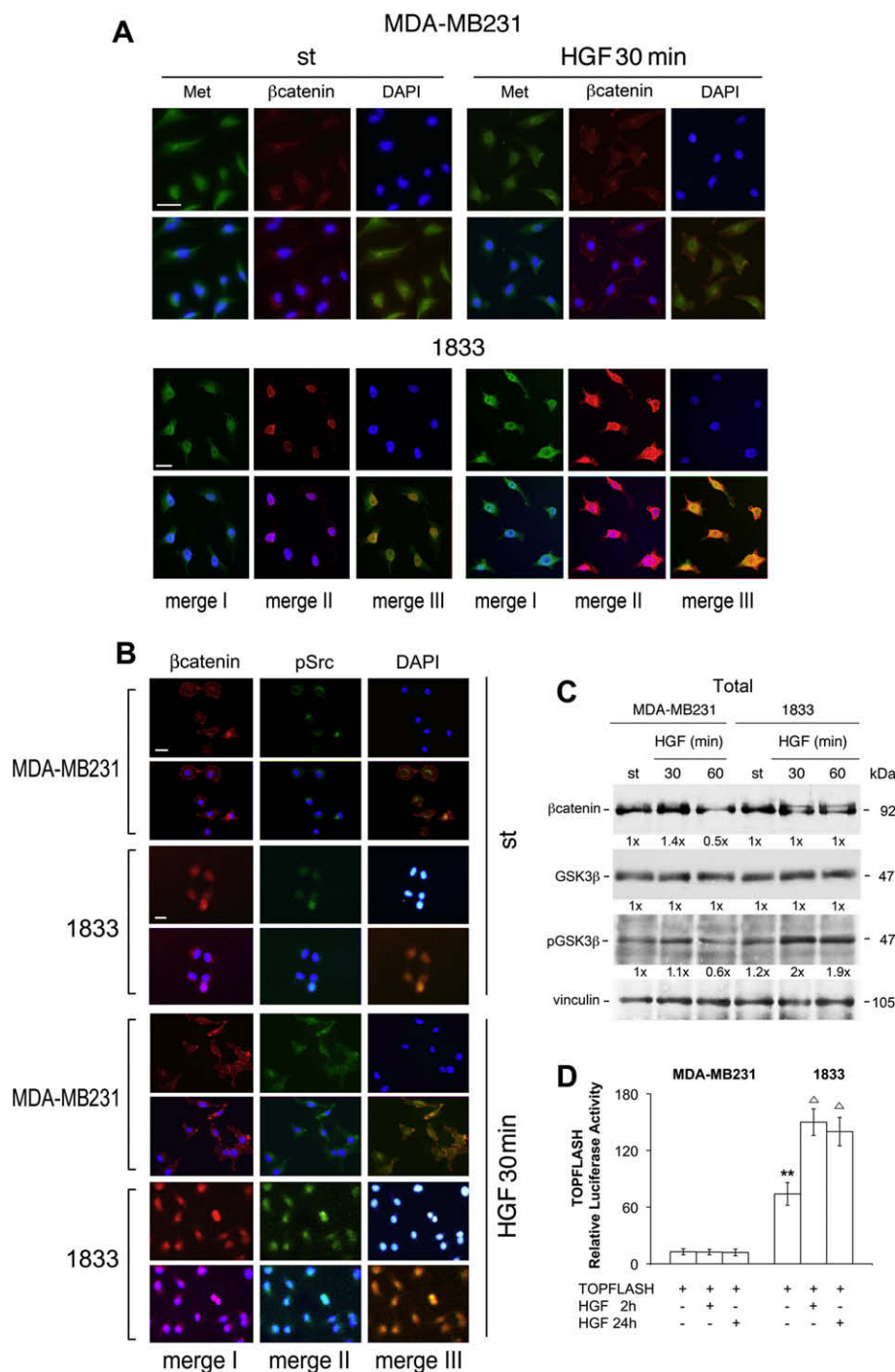


**Fig. 1 – Effect of HGF on  $\beta$ -catenin expression, localisation and TOPFLASH activity.** (A) Immunofluorescence images of cells starved (st), treated with human HGF, and probed with anti-Met (green) and anti- $\beta$ -catenin (red) antibodies. The nuclei were stained with DAPI (blue). Merge I, Met/DAPI; merge II,  $\beta$ -catenin/DAPI; merge III, Met/ $\beta$ -catenin; (B) immunofluorescence images of cells starved (st), treated with human HGF, and probed with anti- $\beta$ -catenin (red) and anti-phospho-c-Src (pSrc, green) antibodies. The nuclei were stained with DAPI (blue). Merge I,  $\beta$ -catenin/DAPI; merge II, pSrc/DAPI; merge III,  $\beta$ -catenin/pSrc. For (A) and (B) the images are taken at 400X magnification, and are representative of experiments performed in triplicate. Size bars in the upper panels: MDA-MB231 cells, 50  $\mu$ m; 1833 cells, 45  $\mu$ m. (C) The numbers at the bottom of Western blots indicate the fold-variations versus st-MDA-MB231 cells, taken as 1. Vinculin was used for normalisation. The experiments have been repeated three times with similar results. (D) The cells, transiently transfected with TOPFLASH-gene reporter, were treated with HGF. The histograms indicate the Firefly/Renilla luciferase activity ratios. The data are the means  $\pm$  SE of five independent experiments performed in triplicate. \*\*P < 0.005 versus st-MDA-MB231 cells;  $\triangle$ P < 0.05 versus st-1833 cells.



As shown in Fig. 1C, 60 min-HGF treatment of MDA-MB231 cells reduced (~50%)  $\beta$ -catenin level while in 1833 cells HGF did not affect  $\beta$ -catenin level, but phosphorylated  $\beta$ -catenin migrating, in fact, as a couple of bands. The Ser9-phosphorylated form of GSK3 $\beta$  also increased (2-fold) in HGF-treated 1833 cells, while decreasing (~40%) in MDA-MB231 cells 60 min after HGF. GSK3 $\beta$  protein levels were unmodified by HGF treatment in both the cell lines. Thus,  $\beta$ -catenin was stabilised by HGF in 1833 cells because of degradation impairment, as consequence of GSK3 $\beta$ -serine phosphorylation that inactivates the enzyme.<sup>29</sup>

Finally, MDA-MB231 and 1833 cells were transiently transfected with TOPFLASH-gene reporter containing multiple TCF/LEF consensus sites, upstream of a c-fos minimal promoter driving luciferase expression, widely used as an index of  $\beta$ -catenin activity<sup>27</sup> (Fig. 1D). The activity of FOPFLASH, a construct lacking functional TCF/LEF consensus sites and therefore  $\beta$ -catenin independent,<sup>27</sup> was also tested. Under starvation, TOPFLASH activity was about 6-fold higher in 1833 than in MDA-MB231 cells, while FOPFLASH activity was undetectable. Only in 1833 cells, 2 h- and 24 h-HGF treatment enhanced about 2-fold TOPFLASH activity. Noticeably, the luciferase activity was 20-fold lower in non-invasive MCF-7 than in invasive MDA-MB231 breast-cancer cells (data not shown), indicating a relationship of  $\beta$ -catenin/Wnt pathway with aggressiveness.

The elevated TOPFLASH activity in the starved 1833 cells confirmed that  $\beta$ -catenin was constitutively active, and the HGF-dependent increase was due to  $\beta$ -catenin stabilisation and transcriptional control of  $\beta$ -catenin itself at 2 and 24 h, respectively.

### 3.2. $\beta$ -Catenin was activated by tyrosine phosphorylation in 1833 cells

We further clarified the molecular mechanisms involved in  $\beta$ -catenin phosphorylation under our experimental conditions through interaction with Met and/or pSrc. Met basal levels were similarly elevated in 1833 clone and parental MDA-MB231 cells, as demonstrated in immunoprecipitates (IP) with anti-Met antibody (Fig. 2A). The Met receptor levels in these cells are remarkably higher than in MCF-7 cells.<sup>13</sup> In HGF-treated MDA-MB231 cells Met underwent down-regulation (~60% to ~90%), showing a transient increase (1.4-fold) in tyrosine phosphorylation (pTyr) at 30 min, index of receptor activation (pTyr/Met ratio = 3.5). Differently, in 1833 cells the level of Met remained unchanged during all the observation period, Met was phosphorylated by HGF at 30–60 min (pTyr/Met ratio = 2), and co-immunoprecipitated with pSrc at 60 min. However, as shown by immunoprecipitation with anti-c-Src antibody (Fig. 2B), HGF increased c-Src phosphorylation (2- to 3-fold) in the two cell lines and did not modify c-Src levels.

In MDA-MB231 and 1833 cells we evaluated the presence of  $\beta$ -catenin in the immunoprecipitates obtained with anti-Met or anti-c-Src antibody using total extracts. Only in 1833 cells,  $\beta$ -catenin co-immunoprecipitated with c-Src, but not with Met, appearing as faint tyrosine-phosphorylated bands 30–60 min after HGF (Fig. 2B).

IP with anti- $\beta$ -catenin antibody was performed using nuclear extracts (Fig. 2C). After HGF exposure, in 1833 nuclei  $\beta$ -

catenin level and its tyrosine-phosphorylation state increased, and  $\beta$ -catenin co-immunoprecipitated with tyrosine-phosphorylated Met, pSrc and Kank. In contrast, after HGF in MDA-MB231 nuclei tyrosine phosphorylation of  $\beta$ -catenin decreased (~50%) but  $\beta$ -catenin level was unaffected. IP with anti-Met antibody was also performed (Fig. 2D). Met was a 60 kDa COOH-fragment highly tyrosine phosphorylated mostly in 1833-cell nuclei, as shown with the antibodies anti-pTyr and anti-phospho-Met 1234/35 (tyrosines of catalytic site) antibodies. In the immunoprecipitates with total-protein extracts, we detected a 60 kDa band corresponding to Met fragment of nuclear origin.<sup>24</sup>

### 3.3. Human-breast cancer cells metastatised to bones

Representative images of whole body dorsal and ventral views by BLI are shown (Fig. 3A). Bone metastases developed in 100% of the mice injected with 1833/TGL cells: the luminescent signal appeared at 10–12 d in the area of the hind limbs, and became well detectable at day 20, further increasing from day 20 to day 28, as indicated by the relative colour map. No luminescent signal was observed in controls. The mice were sacrificed before showing distress and fatal cachexia. During the experimental period, animals were scanned with  $\mu$ -CT to evaluate the presence of osteolysis, that was remarkable at day 28 in metastasis bearing mice (Fig. 3B), co-localising with bioluminescence.

As shown in Fig. 3C (a–c), H&E staining of sections indicated that 1833 metastatic cells prevalently colonised near the growth plate, because adjacent metaphysis are predominantly composed of trabecular bone and are surrounded by hemopoietic marrow, fatty marrow and blood vessels.<sup>31</sup> The bone-marrow cavity of hind limbs was extensively invaded by metastatic cells both at days 20 and 28. Metastasis formation was further demonstrated by positive immunoreactivity with the antibody anti-cytokeratins: the control mice were negative (Fig. 3C [d]).

Our 1833-clone xenograft model was consistent with that of Massagué,<sup>7</sup> who shows also that parental MDA-MB231 cells give bone metastases slowly (10–12 weeks) and in a very low percentage of mice.

### 3.4. Met and $\beta$ -catenin in human-breast cancer metastasis

To deepen the knowledge of the role of HGF/Met system *in vivo*, we investigated Met and  $\beta$ -catenin expression in breast-cancer metastasis. As shown in Fig. 4, Met localised mostly at the plasma membrane of metastatic cells (Tu), showing also cytosolic and nuclear localisations (inset). Met presence in bone metastasis was confirmed by immunoreactivity with the antibody for cytokeratins in serial sections. In all the metastatic mass  $\beta$ -catenin distributed throughout the cells, including the nuclei and perinuclear compartments (inset). No reactivity with the human anti-Met and anti- $\beta$ -catenin antibodies was found in host-mouse tissues.

The data indicated nuclear co-localisation of Met and  $\beta$ -catenin *in vivo*, in agreement with above-reported immunofluorescence and nuclear-immunoprecipitate data.

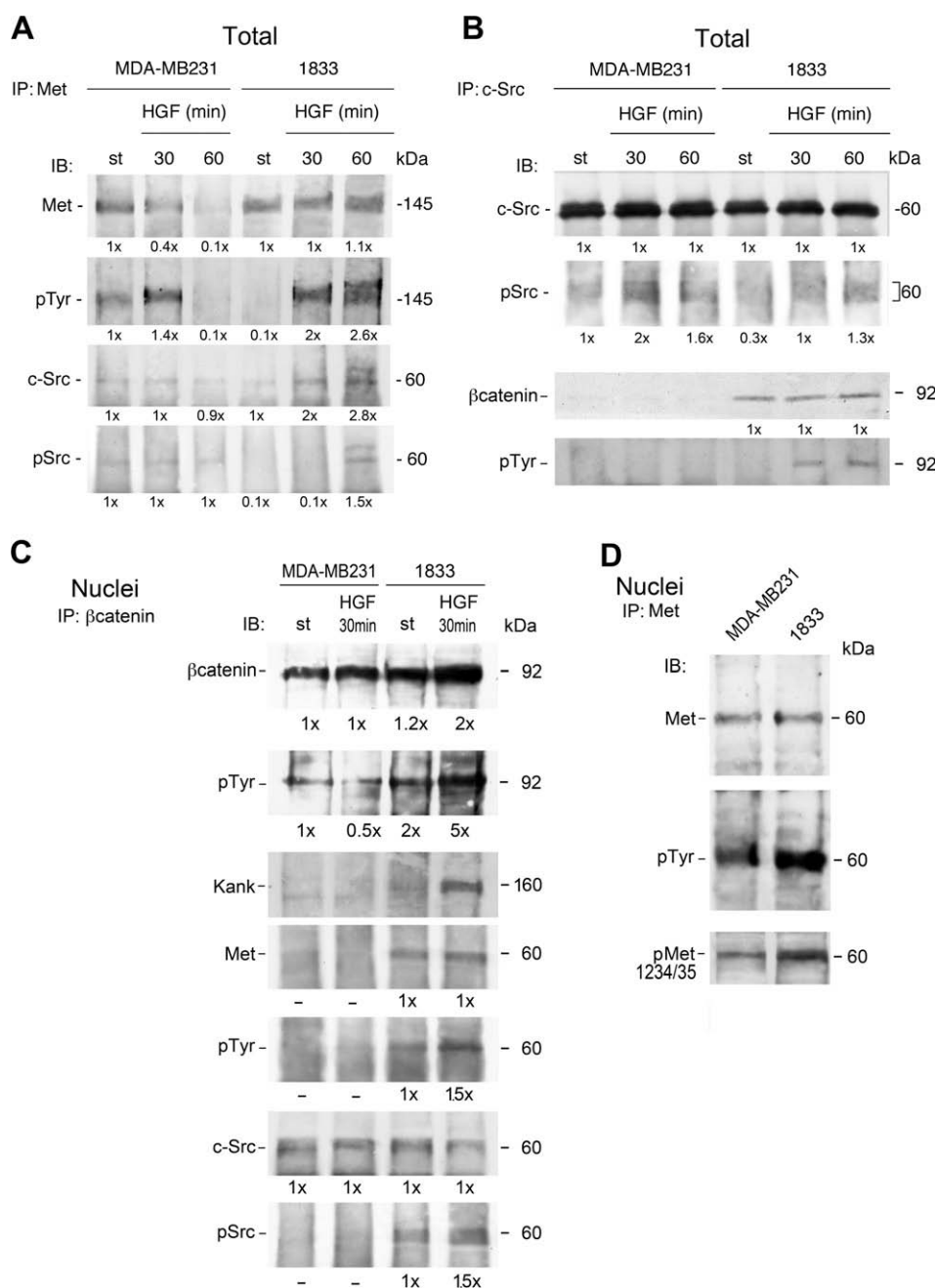


**Fig. 2** – Active Met and c-Src tyrosine kinases were implicated in nuclear  $\beta$ -catenin phosphorylation in 1833 but not in MDA-MB231 cells. Total-protein extracts from cells exposed or not to HGF were immunoprecipitated with the antibody for Met (A) or c-Src (B). The numbers at the bottom indicate the fold-variations versus starved (st)-MDA-MB231 cells, taken as 1.  $\beta$ -Catenin was an exception, being present only in immunoprecipitates from 1833 cells: in this case, st-1833 cells were taken as 1. The experiments have been repeated three times with similar results. Nuclear-protein extracts from MDA-MB231 and 1833 cells exposed or not to HGF, were immunoprecipitated with anti- $\beta$ -catenin (C) or anti-Met (D) antibody. The numbers at the bottom indicate the fold-variations versus st-MDA-MB231 cells, taken as 1. The experiments have been repeated three times with similar results.

### 3.5. HGF production by metastasis and bone microenvironment

To evaluate HGF production in our experimental model of bone metastasis, analyses of human and mouse HGF by immunohistochemistry were performed with specific anti-

bodies. Fig. 5A shows that bone metastases were positive for human HGF, while the mouse-bone marrow cells were negative. The localisation of human HGF was principally cytosolic, as shown in 100 $\times$  magnification of metastatic mass, and in some cells (inset, open arrows) HGF was present also inside the nuclei. These findings were in agreement with the

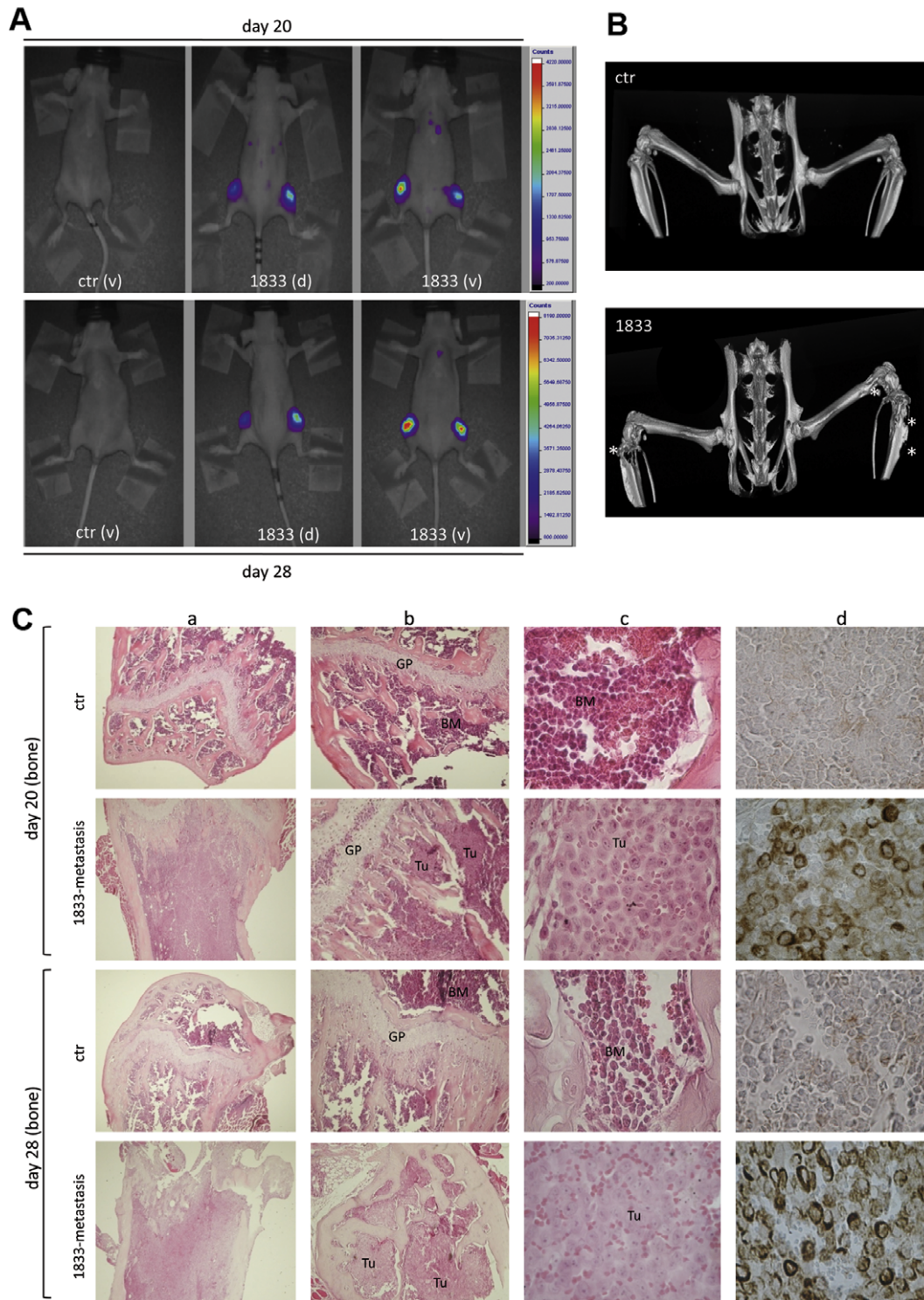


**Fig. 3 – Cells (1833) metastasised to bones. (A)** Representative bioluminescence images of mice injected with 1833/TGL cells or with saline (ctr): ventral (v) and dorsal (d) views. Signals are displayed as pseudo-colour images. **(B)** Representative 3D reconstruction of  $\mu$ CT images at day 28. Asterisks indicate metastasis-induced osteolytic lesions. For **(A)** and **(B)** all the animals in ctr and 1833/TGL groups were monitored at 20 and 28 d. **(C)** H&E staining of sections from ctr and 1833-bone metastases: (a) 4 $\times$ ; (b) 10 $\times$ ; (c) 100 $\times$  magnification; (d) immunohistochemistry for human cytokeratins (100 $\times$  magnification). Representative images of five analysed sections from three different mice are shown. BM, bone marrow; GP, growth plate; Tu, metastatic-tumour growth.

elevated level of HGF in the serum of 20 day-metastasis bearing mice that was  $15.46 \pm 1.85$  ng/ml, while being undetect-

able in the controls. The HGF production *in vitro* by 1833 cells was  $139.2 \pm 15.0$  pg/ml of conditioned medium, corresponding



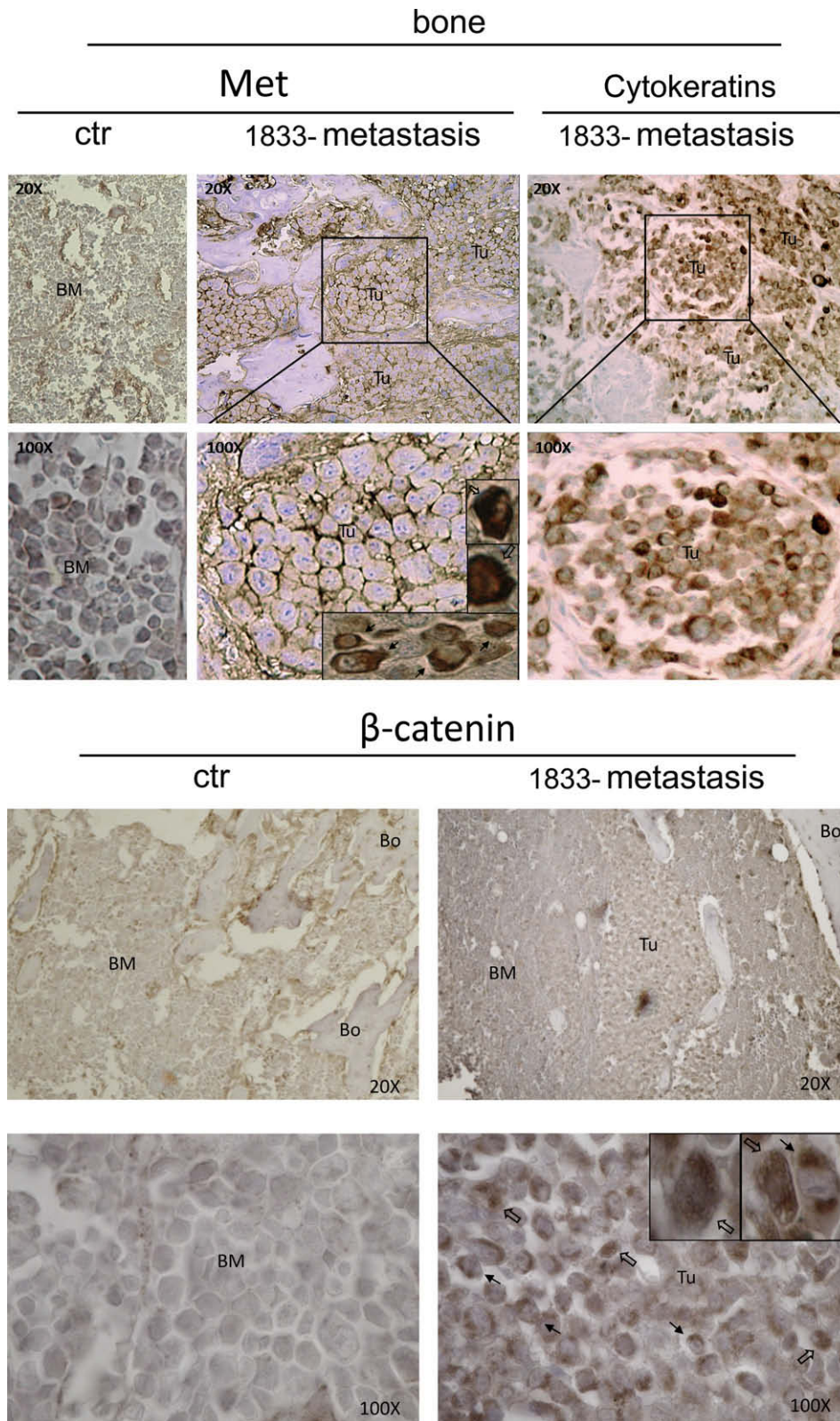


**Fig. 4 – Met and  $\beta$ -catenin in bone metastasis.** Representative-immunohistochemistry analysis of Met and  $\beta$ -catenin in hind-limb sections 20 d after 1833/TGL-cell injection. Five sections from three different mice were analysed with similar results. Also, serial sections for 1833-metastasis were probed with antibody for Met or cytokeratins. Tu, metastatic-tumour growth; Bo, bone tissue; BM, bone marrow. Met 100 $\times$ , Inset, Tu field magnified: black arrows, cytosolic localisation in metastatic cells; open arrows, distribution throughout the metastatic cells including the nuclei.  $\beta$ -catenin 100 $\times$ , Inset, Tu field magnified: black arrows, perinuclear localisation in metastatic cells; open arrows, distribution throughout the metastatic cells including the nuclei.



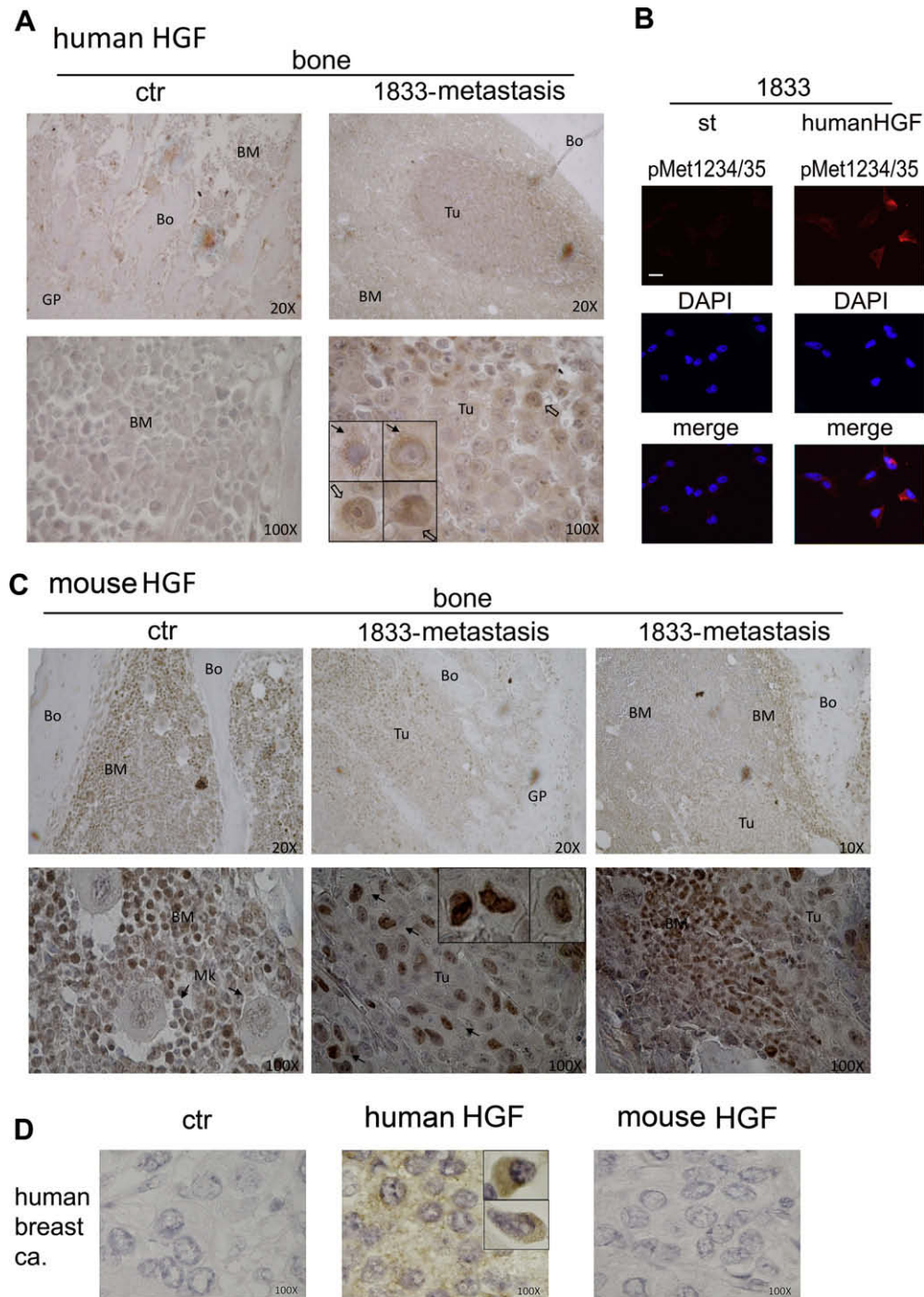


**Fig. 5 – Human and mouse HGF production by bone metastasis and supportive stroma. (A)** Representative-immunohistochemistry analysis with anti-human HGF of hind-limb sections 20 d after 1833/TGL-cell injection. Five sections from three different mice were analysed with similar results. Bo, bone tissue; BM, bone marrow; GP, growth plate; Tu, metastatic-tumour growth. Inset, Tu field magnified: black arrows, cytosolic localisation in metastatic cells; open arrows, distribution throughout the metastatic cells including the nuclei. **(B)** Immunofluorescence images of 1833 cells treated with human HGF, and probed with anti-phospho-Met(tyrosines 1234/1235) antibody (red). The nuclei were stained with DAPI (bleu). The images, taken at 400 $\times$  magnification, are representative of experiments performed in triplicate. Size bar in the upper panel corresponds to 45  $\mu$ m. **(C)** Representative-immunohistochemistry analysis with anti-mouse HGF at day 20. Five sections from three different mice were analysed with similar results. Mk, megakaryocytes. 1833-metastasis panel (Tu), black arrows: metastatic-tumour cells showing mouse HGF inside the nuclei, magnified in the Inset. **(D)** Representative-immunohistochemistry analysis of human-breast carcinoma specimens using anti-human or anti-mouse HGF. ctr, sections without reaction with specific antibodies. Three serial sections were examined with similar results.

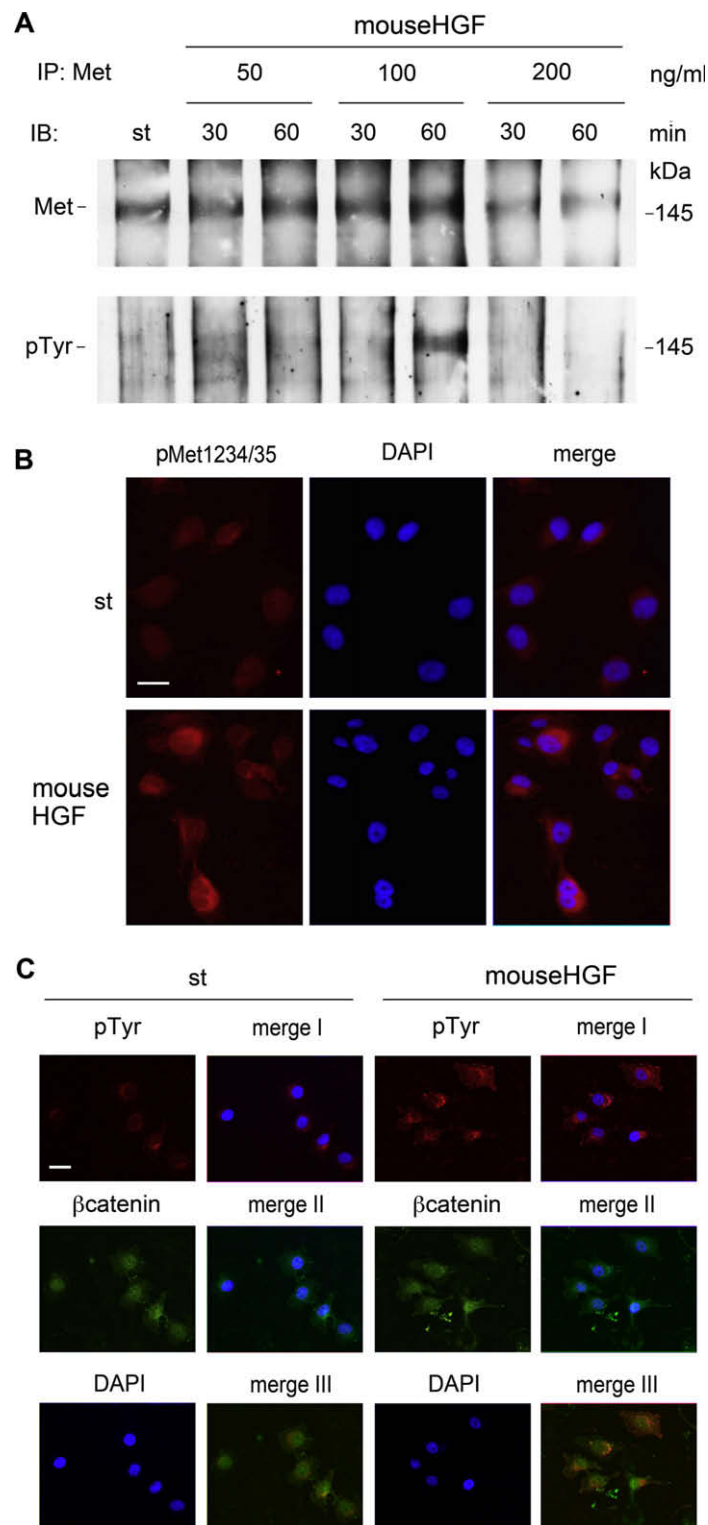


**Fig. 6** – Interaction of mouse HGF with human 1833 metastatic cells. (A) Total protein extracts from starved (st)-1833 cells exposed to various doses of mouse HGF were immunoprecipitated with anti-Met antibody. The experiments have been repeated three times with similar results. Immunofluorescence images of st-1833 cells, treated with mouse HGF (100 ng/ml for 60 min), and probed (B) with anti-phospho-Met(tyrosines 1234/1235) antibody, or (C) with anti-phosphotyrosine (pTyr) (red) and anti- $\beta$ -catenin (green) antibodies. The nuclei were stained with DAPI (bleu). For (C) merge I, pTyr/DAPI; merge II,  $\beta$ -catenin/DAPI; merge III, pTyr/ $\beta$ -catenin. The images, taken at 400X magnification, are representative of experiments performed in triplicate. Size bars in the upper panels correspond to 45  $\mu$ m.

to  $12 \times 10^6$  cells. As shown in Fig. 5B, treatment of 1833 cells with recombinant-human HGF (30 min) enhanced Met-tyrosine phosphorylation (pMet1234/35) throughout the cell, suggesting that HGF might activate the catalytic site of Met. For technical reasons of bone-sample preparation, that does not preserve protein phosphorylation, we could not reproduce this result *in vivo* with immunohistochemistry.

As shown in Fig. 5C, control-bone marrow cells strongly reacted with anti-mouse HGF and, surprisingly, metastatic-cell nuclei were also stained for mouse HGF. This cytokine seemed to be produced by host supportive cells in microenvironmental sites of bone marrow, adjacent to the metastatic mass. HGF, stored as precursor in the bone matrix, might be acti-

vated at the metastatic-cell surface, probably entering in association with Met receptor inside the nuclei.

To confirm the specificity of the antibodies used, human-breast cancer specimens were immunostained with anti-human or anti-mouse HGF (Fig. 5D). Only anti-human HGF gave a positive reaction with the human-tumour preparation.

### 3.6. Mouse HGF activated Met in human 1833 metastatic cells

To give further proof of the interaction of mouse HGF with human-metastatic cells, and in view of the homology (more than 90%) with human HGF,<sup>32</sup> we treated 1833 cells with various doses of recombinant-mouse HGF evaluating by immunoprecipitation human Met activation through tyrosine phosphorylation (pTyr) (Fig. 6A). Recombinant-mouse HGF was maximally effective at 100 ng/ml after 60 min causing Met phosphorylation. This was confirmed by immunofluorescence experiments, in which 60 min-treatment of 1833 cells with mouse HGF (100 ng/ml) enhanced pMet 1234/35 signal at nuclear and perinuclear level (Fig. 6B). A scatter effect was also observed (data not shown).

Further, using mouse HGF (100 ng/ml) for 60 min we observed by immunofluorescence an enhancement of pTyr signal, that co-localised with  $\beta$ -catenin in nuclear and perinuclear compartments (Fig. 6C), and by TOPFLASH transfection a 2-fold increase in luciferase activity (data not shown).

### 3.7. 1833 Bone metastatic clone strongly differed from parental MDA-MB231 cells for $\beta$ -catenin/Wnt pathway activity and the response to HGF

Fig. 7 schematises the principal differences in the molecular pathways studied between 1833-bone metastatic clone and parental MDA-MB231 cells (panel A), and the interactions of human and mouse HGF with bone metastasis (panel B).

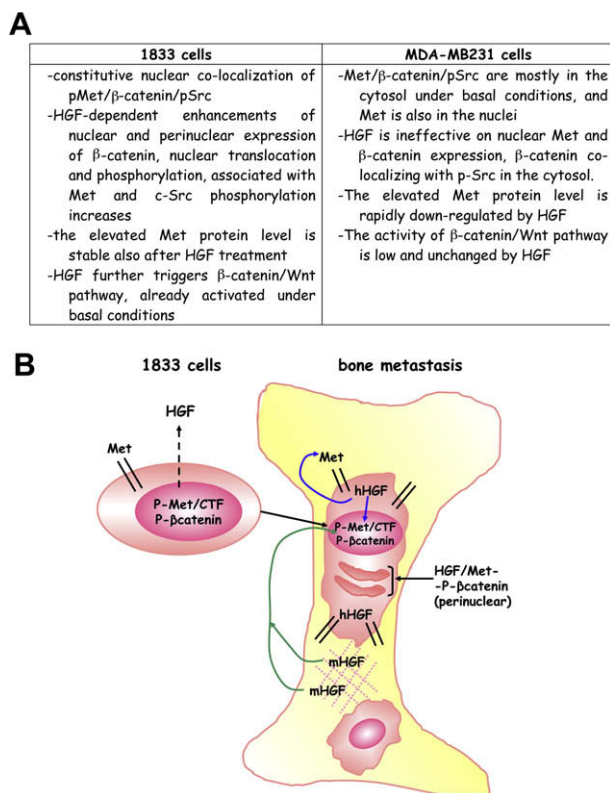


**Fig. 7 – (A) Principal differences between 1833 clone and parental MDA-MB231 cells as regards HGF/Met and  $\beta$ -catenin/Wnt pathways. (B) Scheme of Met activation in bone metastasis by HGF of double origin, human-tumour and mouse-bone marrow, and relationship with  $\beta$ -catenin-phosphorylative activation in nuclear and perinuclear (cytosol) compartments. Bone metastasis produced HGF that possibly caused phosphorylative activation of Met in autocrine/intracrine manner, occurring at cell membrane and nuclear level. Mouse HGF, produced by bone-marrow supportive cells, entered metastatic cell nuclei, possibly activating Met-CTF. The presence of nuclear  $\beta$ -catenin in metastasis indicated translocation from cytosol and activation that might be the consequence of tyrosine phosphorylation via HGF/Met. In 1833 cells *in vitro* nuclear Met-CTF as well as  $\beta$ -catenin were constitutively phosphorylated, and were responsive to HGF. CTF, COOH-terminal fragments of Met; hHGF, human HGF; mHGF, mouse HGF.**

## 4. Discussion

Here, we generated a model suitable to study the role of HGF/Met system in osteolytic metastatic process of breast carcinoma. Met, that was remarkably expressed in 1833-cell line as full-length receptor and as a nuclear-tyrosine phosphorylated 60 kDa fragment, in bone metastases *in vivo* localised at plasma-membrane level as well as inside the cells, including the nucleus. The Met receptor in the metastases probably underwent autocrine/intracrine activation by HGF, localised in the cytosol and the nuclei. Consistently, serum-human HGF was elevated in metastasis bearing mice, but not in 1833 cell-conditioned medium.

These data are very important and new because with the exception of primary sarcomas and gliomas, solid tumours rarely produce HGF.<sup>22</sup> The synthesis of HGF seemed to occur in human-breast cancer and the xenograft metastatic model, suggesting the possibility to block this pathway *in vivo*. In our xenograft metastatic model, HGF production by human-metastatic cells after bone engraftment might concomitantly activate cell membrane and nuclear Met receptor in agreement with *in vitro* experiments.



In bone metastases we observed abnormal localisation of  $\beta$ -catenin in nuclear and perinuclear (cytosolic) compartments. Similar localisation correlates with malignant progression at invasive front of colon-carcinoma metastases. Only in brain metastases of colon carcinoma but not in primary meningiomas,  $\beta$ -catenin shows nuclear localisation.<sup>8,10</sup> Nuclear immunoreactivity in bone metastases indicates  $\beta$ -catenin translocation from cytoplasmic compartments to the nucleus related to its function in TCF transactivation.<sup>10</sup>

The regulation of  $\beta$ -catenin levels/function in breast cancer metastasis was complex being affected by HGF and might depend on the step of metastatisation, related to the shift between epithelial-mesenchymal transition (EMT) and mesenchymal-epithelial transition (MET) typical of metastases.<sup>14,15</sup>  $\beta$ -catenin seemed to be constitutively tyrosine-phosphorylated and activated in the nuclear compartment by phospho-Met and phospho-c-Src. This mechanism(s) might represent a big advantage for metastatic cells, considering that during their long life they often do not interact with tumour microenvironment. However, after the arrival of metastatic cells to the secondary site, HGF produced by bone marrow might further enhance  $\beta$ -catenin-TCF transactivation by increasing  $\beta$ -catenin phosphorylation and the translocation from the cytosolic compartment(s) to the nucleus, possibly favoured by Kank.<sup>33</sup> HGF-dependent inactivation of GSK3 $\beta$  in 1833 cells seemed to participate in  $\beta$ -catenin stabilisation,<sup>29,34</sup> and activation of  $\beta$ -catenin promoter by HGF increased protein level. It is worth noting that only in 1833, but not in parental MDA-MB231 cells, COOH-Met fragments phosphorylated by HGF were associated with phospho- $\beta$ -catenin, possibly participating in the regulation of  $\beta$ -catenin-TCF transcriptional activity. In 1833 metastatic cells, Met was probably internalised by HGF and entered the Golgi vesicles, where it might be cleaved into COOH-fragment,<sup>24,35</sup> co-localising with  $\beta$ -catenin. We suggest that in the perinuclear compartment  $\beta$ -catenin was tyrosine phosphorylated by HGF/COOH-Met system, and then stabilised and activated thus accumulating in the nucleus, to trigger specific signals for growth and invasion.<sup>36</sup>

The gene signature associated with poor prognosis facilitates the emergence of metastatic cells in the primary tumour, but the specific set of genes associated with bone metastases is responsible for the cellular activities necessary for metastatisation.<sup>7</sup> In addition, the metastatic capacity has been suggested as a late, acquired event in tumourigenesis and during secondary growth, through epigenetic control of transcription.<sup>1,13,22</sup> The TOPFLASH activity was remarkably higher in 1833 clone than in parental MDA-MB231 cells, and was stimulated by HGF. Considering the panel of genes regulated by  $\beta$ -catenin-TCF,<sup>12,17–19</sup> this pathway might regulate various steps of the metastatic process under the influence of HGF/Met, including growth, invasiveness and osteolysis. Our breast-cancer metastatic model with a critical role of  $\beta$ -catenin-TCF, substantially differed from the  $\beta$ -cell carcinogenesis mouse model, characterised by low level of  $\beta$ -catenin without nuclear localisation.<sup>37</sup>

Altogether our findings support the hypothesis that continuous and dynamic turnover of the bone matrix and bone marrow provides a fertile ground for breast-cancer metastatic

cells. HGF seemed to be produced by stromal cells and osteoblasts of mouse-bone marrow, originating from mesenchymal stem cells, adjacent to the metastases.<sup>21,38</sup> The bone-marrow mesenchymal cells may constitute a 'pre-metastatic niche' that facilitates tumour cell growth in distant organs.<sup>9,31</sup> c-Src-dependent CXCL12 survival signal in the bone marrow microenvironment favours 1833 metastatic growth.<sup>39</sup>

The mouse HGF from the host-bone marrow entered the nuclei of human-metastatic cells, possibly activating signalling pathways downstream of Met. Differences with previous data<sup>22</sup> might depend on the model used, because 1833 cells seemed to be particularly responsive to HGF, in relation to the plasticity of metastatic cell phenotype. The dual-species nature of the present model allowed us to monitor HGF of human-neoplastic origin from mouse-stromal source. Different intracellular Met-traffic-related pathways might be utilised by HGF of tumour-intracrine origin and by mouse-paracrine HGF (see Fig. 7).

At a difference with parental MDA-MB231 cells, bone metastatic 1833 clone was largely sensitive to microenvironmental stimuli such as HGF. Nuclear COOH-Met probably enhanced transduction signalling generated at plasma membrane by full-length Met that seemed persistently phosphorylated by HGF in 1833 cells. In contrast, in MDA-MB231 cells full-length Met was down-regulated by HGF and transiently phosphorylated. Neither in 1833 nor in MDA-MB231 cells full-length Met co-precipitated with  $\beta$ -catenin, thus differing from hepatocytes where plasma membrane Met phosphorylates  $\beta$ -catenin.<sup>40</sup>

In conclusion, realising that the contribution to human-breast cancer metastases of the Wnt pathway, under the influence of bone microenvironment, was surprisingly untested<sup>3</sup>, we clarified that HGF/Met/pSrc/ $\beta$ -catenin-TCF signalling pathways were coordinately regulated possibly playing a role in bone-metastatic progression. Progression occurs through micrometastases undergoing complex genetic, epigenetic and resultant transcriptional changes.<sup>22</sup> Therefore, the development of therapies that can disrupt this signalling network holds great promise because of the possibility to affect the aggressive phenotype.<sup>4</sup> Moreover, a better understanding of the role of these pathways in bone arrest/colonisation will help in defining early treatments which could be effective in delaying bone metastasis formation.

---

## Conflict of interest statement

None declared.

---

## Acknowledgements

We are grateful to Dr. Joan Massagué (Memorial Sloan-Kettering Cancer Center, New York) for the 1833-bone metastatic clone, the parental MDA-MB231 and the 1833/TGL cells. This work was supported by Ministero Istruzione-Università-Ricerca PRIN 2007-12-25201001-14; Ministero Salute: Ricerca Finalizzata-RF 06-81, Ricerca Corrente-4029; Italian Association for Cancer Research.

## REFERENCES

- Kopfstein L, Christofori G. Metastasis: cell-autonomous mechanisms versus contributions by the tumour microenvironment. *Cell Mol Life Sci* 2006;**63**:449–68.
- Kingsley LA, Fournier PG, Chirgwin JM, Guise TA. Molecular biology of bone metastasis. *Mol Cancer Ther* 2007;**6**:2609–17.
- Iiizumi M, Liu W, Pai SK, Furuta E, Watabe K. Drug development against metastasis-related genes and their pathways: a rationale for cancer therapy. *Biochim Biophys Acta* 2008;**1786**:87–104.
- Eder JP, Vande Woude GF, Boerner SA, LoRusso PM. Novel therapeutic inhibitors of the c-Met signaling pathway in cancer. *Clin Cancer Res* 2009;**15**:2207–14.
- Benvenuti S, Comoglio PM. The MET receptor tyrosine kinase in invasion and metastasis. *J Cell Physiol* 2007;**213**:316–25.
- Desiderio MA. Hepatocyte growth factor in invasive growth of carcinomas. *Cell Mol Life Sci* 2007;**64**:1341–54.
- Kang Y, Siegel PM, Shu W, et al. A multigenic program mediating breast cancer metastasis to bone. *Cancer Cell* 2003;**3**:537–49.
- Bandapalli OR, Dihlmann S, Helwa R, et al. Transcriptional activation of the beta-catenin gene at the invasion front of colorectal liver metastases. *J Pathol* 2009;**218**:370–9.
- Barnhart BC, Simon MC. Metastasis and stem cell pathways. *Cancer Metastasis Rev* 2007;**26**:261–71.
- Brunner EC, Romeike BF, Jung M, Comtesse N, Meese E. Altered expression of beta-catenin/E-cadherin in meningiomas. *Histopathology* 2006;**49**:178–87.
- Wang L, Liu T, Wang Y, et al. Altered expression of desmocollin 3, desmoglein 3, and beta-catenin in oral squamous cell carcinoma: correlation with lymph node metastasis and cell proliferation. *Virchows Arch* 2007;**451**:959–66.
- Hall CL, Keller ET. The role of Wnts in bone metastases. *Cancer Metastasis Rev* 2006;**25**:551–8.
- Ridolfi E, Matteucci E, Maroni P, Desiderio MA. Inhibitory effect of HGF on invasiveness of aggressive MDA-MB231 breast carcinoma cells, and role of HDACs. *Br J Cancer* 2008;**99**:1623–34.
- Bendinelli P, Matteucci E, Maroni P, Desiderio MA. NF- $\kappa$ B activation, dependent on acetylation/deacetylation, contributes to HIF-1 activity and migration of bone metastatic breast cancer cells. *Mol Cancer Res* 2009;**7**:1328–41.
- Min C, Eddy SF, Sherr DH, Sonenshein GE. NF- $\kappa$ B and epithelial to mesenchymal transition of cancer. *J Cell Biochem* 2008;**104**:733–44.
- Kizaka-Kondoh S, Itasaka S, Zeng L, et al. Selective killing of hypoxia-inducible factor-1-active cells improves survival in a mouse model of invasive and metastatic pancreatic cancer. *Clin Cancer Res* 2009;**15**:3433–41.
- Marchenko ND, Marchenko GN, Weinreb RN, et al. Beta-catenin regulates the gene of MMP-26, a novel metalloproteinase expressed both in carcinomas and normal epithelial cells. *Int J Biochem Cell Biol* 2004;**36**:942–56.
- El-Tanani MK, Campbell FC, Kurisetty V, et al. The regulation and role of osteopontin in malignant transformation and cancer. *Cytokine Growth Factor Rev* 2006;**17**:463–74.
- Gavert N, Sheffer M, Raveh S, et al. Expression of L1-CAM and ADAM10 in human colon cancer cells induces metastasis. *Cancer Res* 2007;**67**:7703–12.
- Matsumoto K, Nakamura T. Hepatocyte growth factor and the Met system as a mediator of tumour-stromal interactions. *Int J Cancer* 2006;**119**:477–83.
- Ono K, Kamiya S, Akatsu T, et al. Involvement of hepatocyte growth factor in the development of bone metastasis of a mouse mammary cancer cell line, BALB/c-MC. *Bone* 2006;**39**:27–34.
- Knudsen BS, Vande Woude G. Showering c-MET-dependent cancers with drugs. *Curr Opin Genet Dev* 2008;**18**:87–96.
- Chen HH, Su WC, Lin PW, Guo HR, Lee WY. Hypoxia-inducible factor-1 $\alpha$  correlates with MET and metastasis in node-negative breast cancer. *Breast Cancer Res Treat* 2007;**103**:167–75.
- Matteucci E, Bendinelli P, Desiderio MA. Nuclear localization of active HGF receptor Met in aggressive MDA-MB231 breast carcinoma cells. *Carcinogenesis* 2009;**30**:937–45.
- Ponomarev V, Doubrovina M, Serganova I, et al. A novel triple-modality reporter gene for whole-body fluorescent, bioluminescent, and nuclear noninvasive imaging. *Eur J Nucl Med Mol Imaging* 2004;**31**:740–51.
- Tacchini L, Dansi P, Matteucci E, Desiderio MA. Hepatocyte growth factor signalling stimulates hypoxia inducible factor-1 (HIF-1) activity in HepG2 hepatoma cells. *Carcinogenesis* 2001;**22**:1363–71.
- Matteucci E, Ridolfi E, Desiderio MA. Hepatocyte growth factor differently influences Met-E-cadherin phosphorylation and downstream signaling pathway in two models of breast cells. *Cell Mol Life Sci* 2006;**63**:2016–26.
- Wallenius V, Hisaoka M, Helou K, et al. Overexpression of the hepatocyte growth factor (HGF) receptor (Met) and presence of a truncated and activated intracellular HGF receptor fragment in locally aggressive/malignant human musculoskeletal tumours. *Am J Pathol* 2000;**156**:821–9.
- Papkoff J, Aikawa M. WNT-1 and HGF regulate GSK3 activity and -catenin signaling in mammary epithelial cells. *Biochem Biophys Res Commun* 1998;**247**:851–8.
- Lilien J, Balsamo J. The regulation of cadherin-mediated adhesion by tyrosine phosphorylation/dephosphorylation of beta-catenin. *Curr Opin Cell Biol* 2005;**17**:459–65.
- Bussard KM, Gay CV, Mastro AM. The bone microenvironment in metastasis; what is special about bone? *Cancer Metastasis Rev* 2008;**27**:41–55.
- Tashiro K, Hagiya M, Nishizawa T, et al. Deduced primary structure of rat hepatocyte growth factor and expression of the mRNA in rat tissues. *Proc Natl Acad Sci USA* 1990;**87**:3200–4.
- Wang Y, Kakinuma N, Zhu Y, Kiyama R. Nucleo-cytoplasmic shuttling of human Kank protein accompanies intracellular translocation of beta-catenin. *J Cell Sci* 2006;**119**:4002–10.
- Huang H, He X. Wnt/beta-catenin signaling: new (and old) players and new insights. *Curr Opin Cell Biol* 2008;**20**:119–25.
- Kermorgant S, Zicha D, Parker PJ. Protein kinase C controls microtubule-based traffic but not proteasomal degradation of c-Met. *J Biol Chem* 2003;**278**:28921–9.
- Gasparoni A, Chaves A, Fonzi L, et al. Subcellular localization of beta-catenin in malignant cell lines and squamous cell carcinomas of the oral cavity. *J Oral Pathol Med* 2002;**31**:385–94.
- Herzig M, Savarese F, Novatchkova M, Semb H, Christofori G. Tumour progression induced by the loss of E-cadherin independent of beta-catenin/Tcf-mediated Wnt signaling. *Oncogene* 2007;**26**:2290–8.
- Kucia M, Reza R, Jala VR, et al. Bone marrow as a home of heterogeneous populations of nonhematopoietic stem cells. *Leukemia* 2005;**19**:1118–27.
- Zhang XH, Wang Q, Gerald W, et al. Latent bone metastasis in breast cancer tied to Src-dependent survival signals. *Cancer Cell* 2009;**16**:67–78.
- Monga SP, Mars WM, Padiaditakis P, et al. Hepatocyte growth factor induces Wnt-independent nuclear translocation of beta-catenin after Met-beta-catenin dissociation in hepatocytes. *Cancer Res* 2002;**62**:2064–71.